The LINNEAN SOCIETY of London ZOOLOGICAL Journal of the Linnean Society

Zoological Journal of the Linnean Society, 2013, **169**, 235–250. With 6 figures

Cranial ontogeny in the Puma lineage, *Puma concolor*, *Herpailurus yagouaroundi*, and *Acinonyx jubatus* (Carnivora: Felidae): a three-dimensional geometric morphometric approach

VALENTINA SEGURA[1]*, FRANCISCO PREVOSTI[1] and GUILLERMO CASSINI[1,2]

[1]*División Mastozoología, Museo Argentino de Ciencias Naturales Bernardino Rivadavia, Consejo Nacional de Investigaciones Científicas y Técnicas (CONICET), Buenos Aires, Argentina*
[2]*Departamento de Ciencias Básicas, Universidad Nacional de Luján, Luján, Buenos Aires, Argentina*

Received 5 January 2013; revised 24 April 2013; accepted for publication 24 April 2013

The Puma lineage is a monophyletic group that includes three living species: *Puma concolor*, *Herpailurus yagouaroundi*, and *Acinonyx jubatus*. It has been analysed from ecological and taxonomic perspectives, but their cranial ontogeny has been poorly studied. In this study, we assessed the cranial shape and size variation through three-dimensional geometric morphometric techniques, and explored the acquisition of definitive shape and size in relation to key life-history events. Each species occupied different locations in the shape morphospace: *A. jubatus* and *P. concolor* showed shorter and wider skulls, with more expanded zygomatic arches, than *H. yagouaroundi*, which presented the most divergent pattern of change. Ontogeny was more similar between *P. concolor* and *A. jubatus* than between the closely related *P. concolor* and *H. yagouaroundi*. The evolution of ontogenetic change in the lineage seems to be more influenced by size. Changes detected between juvenile and adult skulls enhanced predatory skills, coincident with the change from a diet of milk to a carnivorous diet. Change patterns suggest that the skull is not morphologically conservative in the lineage, in contrast with other carnivores such as canids and hyaenids. The enlargement of the rostrum observed in some canids and the reinforcement of the bite mechanism of hyaenids were not detected in this group.

doi: 10.1111/zoj.12047

ADDITIONAL KEYWORDS: allometry – development – felidae – growth – morphology – skull.

INTRODUCTION

The family Felidae is composed of diverse species, with notable variation in size, including large species such as *Panthera tigris*, 90–258 kg, as well as small cats like *Leopardus guigna*, 1.7–3 kg (Mazák, 1981; Sunquist & Sunquist, 2009). However, extant felids are considered morphologically homogeneous among carnivores with regards to their adult cranial morphology and function (Goswami, 2006; Sunquist & Sunquist, 2009; Sicuro, 2011). A possible cause of this uniformity is, on one hand, the relatively young age of this group (Late Miocene), and on the other hand, their highly specialized predatory habit, related to their ecomorphological role as hypercarnivores. According to some authors (e.g. Holliday & Steppan, 2004; Johnson *et al*., 2006; Figueirido *et al*., 2011), such ecological specialization could generate a decrease in variation and diversity. Associated with a strictly carnivorous diet, adult felids share craniodental characters, i.e. short face, anteriorly oriented orbits, large temporal fossa, large canines, specialized carnassials, and greatly reduced non-carnassial postcanines (Radinsky, 1981; Kitchener, 1991; Giannini *et al*., 2010).

The Puma lineage is a monophyletic clade, supported by both morphological and molecular evidence, that includes three extant species: *Puma concolor*, *Herpailurus yagouaroundi*, and *Acinonyx jubatus* (Salles, 1992; Johnson & O'Brien, 1997;

*Corresponding author. E-mail: valu_z@yahoo.com.ar

Bininda-Emonds, Gittleman & Purvis, 1999; Mattern & McLennan, 2000; Johnson *et al*., 2006). They shared a common ancestor about 6.70 Mya (age of divergence estimation based on nuclear and mitochondrial DNA; Johnson *et al*., 2006), although the oldest fossil record (*Acinonyx* sp.) is from 3.8–3.4 Mya (Werdelin *et al*., 2010). An additional extinct genus in the clade, *Miracinonyx*, includes *Miracinonyx trumani* as a sister group of *P. concolor*, according to molecular evidence (Barnett *et al*., 2005), or a sister group of *A. jubatus*, according to morphological evidence (Van Valkenburgh, Grady & Kurtén, 1990; Christiansen & Mazák, 2009). In any case, this apparent contradiction does not modify the relationships between the living taxa considered in this work.

Puma concolor and *H. yagouaroundi* are currently distributed from North to South America, and have an average weight of 53–72 and 3–7.6 kg, respectively. *Acinonyx jubatus* is restricted to Africa and Iran, and has a mean weight of 39–59 kg (O'Brien & Johnson, 2007; Sunquist & Sunquist, 2009). The study of postnatal cranial ontogeny of three closely related felids is interesting, given the potential to show how the suckling young develops the structures and functions of a highly specialized predator. Previous studies about cranial shape and phylogenetic approaches using geometric morphometrics in carnivores have focused on functionality (e.g. Christiansen, 2008; Meloro *et al*., 2008; Prevosti, Turazzini & Chemisquy, 2010; Goswami, Milne & Wroe, 2011), morphological integration (e.g. Goswami, 2006; Figueirido, Tseng & Martín-Serra, 2013), convergence (e.g. Wroe & Milne, 2007; Figueirido *et al*., 2010, 2011; Goswami *et al*., 2011), ecomorphology (e.g. Figueirido & Soibelzon, 2010; Prevosti *et al*., 2010), and evolutionary trends (e.g. Prevosti *et al*., 2010; Sicuro, 2011); however, the patterns of cranial ontogeny in felids have been insufficiently studied. Most of the previous studies have been primarily descriptive, focused on dental eruption, age estimation, and morphological description (e.g. *Panthera onca*, Stehlik, 1971; *Panthera pardus*, Stander, 1997; *Leopardus wiedii*, Volf, 1972; Fagen & Wiley, 1978; Petersen & Petersen, 1978; *P. concolor*, Gay & Best, 1996; Shaw *et al*., 2007; *Lynx* spp., Crowe, 1975; García-Perea, 1996; *A. jubatus*, Broom, 1949; Caro, 1994; *Caracal caracal*, Stuart & Stuart, 1985). In spite of this, Segura & Flores, (2009) and Giannini *et al*. (2010) studied the ontogenetic changes and their functional consequences in *P. concolor*, and Christiansen (2012) studied the nature and magnitude of craniomandibular shape changes during ontogeny in *Smilodon* spp. Other remarkable works in ontogeny include: Wayne (1986), who studied ontogenetic trajectories of skull growth in *Canis familiaris*; Drake (2011) and Drake & Klingenberg (2010), who examined heterochronic patterns in the skull morphology of *C. familiaris*; La Croix *et al*. (2011a, b), who studied the cranial growth and development of *Canis latrans*; and Segura & Prevosti (2012), who explored the ontogenetic changes of *Lycalopex culpaeus*.

The comparative study of the ontogenetic pattern of skull change of these three closely related felid species has never been compared in a comprehensive way. In this work we explore and discuss the variation of skull shape and development in the three living species of the Puma lineage, using three-dimensional geometric morphometrics. We expect to assess the degree of overlap or dissociation in the morphospace depicted by the principal component of interest. We also explore the relationship between skull size and shape for different age stages of the three species in relation to their life history. Because diet exhibits a strong relationship with jaw musculature and skull shape, we expect to detect specific shape changes associated with dietary changes from juvenile to adult. The apparent homogeneous model of the felid skull is approached here from a comparative perspective, considering its variation during growth in these closely related, but morphometrically and ecologically divergent, species.

MATERIAL AND METHODS

Background information

Puma concolor and *A. jubatus* weigh 400 g (Eaton & Verlander, 1977) and 300 g (Krausman & Morales, 2005), respectively, at birth, whereas *H. yagouaroundi* weighs only 136 g (Buzas & Gulyas, 2012). Additionally, the gestation periods of *P. concolor* (82–96 days; Currier, 1983) and *A. jubatus* (90–95 days; Eaton & Verlander, 1977) are longer than that of *H. yagouaroundi* (70–75 days; Breton, 2007). However, the three species reach sexual maturity almost at the same time: between 1 and 2.5 years old (Currier, 1983; Oliveira, 1998; Krausman & Morales, 2005).

Sample

We analysed a sample of 336 specimens representing the three living species of the Puma lineage: *P. concolor* ($N = 110$); *H. yagouaroundi* ($N = 147$); and *A. jubatus* ($N = 79$). The sample includes both juveniles and adults from different age stages, estimated by dental formulae and tooth wear, following a modified version of the classification described by Segura & Prevosti (2012) (Table 1). Our sample included the following juveniles (numbers indicate females, males, and unsexed specimens, respectively) – *P. concolor*, B, 2/0/0; J1, 1/2/5; J2, 0/0/2; J3, 1/0/2; J4, 0/0/3; *H. yagouaroundi*, B, 0/0/1; J1, 4/3/4; J2, 2/0/3; J3, 6/3/2; J4, 3/2/2; *A. jubatus*, B, 0/0/0; J1, 1/1/1; J2, 1/1/0;

Table 1. Age classes estimated by dental formulae and tooth wear (a modified version of the classification of Segura & Prevosti, 2012)

B, deciduous dentition still not erupted (i.e. pre-weaning).
J1, complete deciduous dentition present.
J2, permanent I1, i1, and i2 erupted. With I2, I3, i3, M1, and m1 erupting.
J3, canines, P2, and P4 erupting. With I2, i3, M1 erupted.
J4, definitive incisors, canines, and molars fully erupted. P2 and P4 erupted. With P3, p3, and p4 erupting.
A1, complete permanent dentition with no wear.
A2, complete permanent dentition with slight wear, with blunt cusps of incisors, canines, premolars, and molars.
A3, complete permanent dentition with dentine horns exposed on the cusps of premolars and molars and I3 at the same level that I1 and I2.

J3, 1/1/0; J4, 0/1/1 – and the following adults – *P. concolor*, A1, 7/7/22; A2, 4/5/31; A3, 2/2/12; *H. yagouaroundi*, A1, 13/22/18; A2, 17/12/18; A3, 1/3/8; *A. jubatus*, A1, 9/14/11; A2, 14/9/11; A3, 1/1/0.

The material belongs to the mammal collections of the following institutions (see the Appendix): American Museum of Natural History (AMNH); Colección Félix de Azara (CFA); Colección Mamíferos Lillo (CML); Field Museum of Natural History (FMNH); Museo Argentino de Ciencias Naturales Bernardino Rivadavia (MACN); Museo de La Plata (MLP); National Museum of Natural History, Smithsonian Institution (NMNH).

Landmarks

Thirty-eight cranial landmarks were used to describe the skull. We used landmarks with clear homology to types 1 and 2 (*sensu* Bookstein, 1991), such as tripartite sutures and processes. The landmarks were digitized in three dimensions with a Microscribe MX 6DOF System (GoMeasured3D, Amherst, VA, USA), which has an accuracy of 0.0508 mm and uses optical sensors to measure three-dimensional coordinates, eliminating the problem of non-random errors found in magnetic digitization systems. The landmarks are listed in Table 2 and illustrated in Figure 1. In order to maximize the sample we digitized one half of the skull. To improve the visualization and avoid putative Procrustes alignment artifacts, the hemicranium landmark configuration was reflected in the plane of symmetry defined by sagittal landmarks. To do so, we used the R-function AMP.r written by Annat Haber, University of Chicago (available online at http://life.bio.sunysb.edu/morph/; also see Cassini & Vizcaíno, 2012: Online Resource 1).

Table 2. Definition of the landmarks used in the geometric morphometric analyses

Cranial landmarks
1 Tip of premaxilla in the *sutura interincisiva*
2 Frontal point in the *sutura incisivomaxillaris* at level of dentary row
3 Tip of nasal process
4 Anterior point of the nasals in the *sutura internasalis*
5 Anterior contact of *sutura nasomaxillaris*
6 Posterior contact of *sutura nasomaxillaris*
7 Midline in *Sutura incisivomaxillaris*
8 Midline in *Sutura palatomaxillaris*
9 Point below the infraorbitary foramen at level of dentary row
10 Point below the lacrimal foramen at level of dentary row
11 Lacrimal foramen
12 Apex of *sutura frontomaxillaris*
13 Midline of *sutura frontonasalis*
14 Tip of the supraorbital process
15 Tip of the infraorbital process
16 Point below the infraorbital process in the zygomatic process of jugal
17 Anterior point of temporal fossa
18 Posterior point of dentary row
19 Posterior point of palatine torus
20 Point in the *sutura pterygopalatina*
21 Internal edge of temporal fossa
22 External edge of temporal fossa
23 Tip of postglenoid process
24 Intersection between *sutura coronalis*, *sutura sagittalis*, and *sutura interfrontalis*
25 Apex of the braincase
26 Tip of mastoid process
27 Superior point of external auditory meatus
28 Inferior point of external auditory meatus
29 Apex of tympanic bulla
30 Anterior point of tympanic bulla
31 Internal point of tympanic bulla
32 Posterior point of tympanic bulla
33 Tip of paracondylar process
34 External apex of occipital condyle
35 Internal apex of occipital condyle
36 Inferior point in the foramen magnum
37 Superior point in the foramen magnum
38 Point of the inion

Data analysis

Landmark configurations were superimposed in order to remove the spatial variation that does not correspond to form, using Generalized Procrustes Analysis (GPA; Goodall, 1991; Rohlf, 1999). This procedure minimizes the sum of squared distances between homologous landmarks by translating, rotating, and

scaling them to unit centroid size (Dryden & Mardia, 1998), using the software MORPHOLOGIKA 2 v2.5 (O'Higgins & Jones, 2006). We performed a principal component analysis (PCA), using the same software, to identify the major components of variation in a combined analysis across the Puma lineage, allowing visualization of shape changes based on the position of the taxa in the morphospace, along the principal components (PCs) of interest. The PCA was performed for the three species across all age classes.

To investigate how allometric variation in shape is associated with size, we performed a multivariate regression of the Procrustes coordinates against the log-transformed centroid size. The significance of the regression was tested with a permutation test with 10 000 resamples (Bookstein, 1991; Mitteroecker *et al*., 2004). For comparisons between multivariate regressions of shape on size of the three species, we computed the angles between the corresponding regression vectors. These angles were computed as the arccosines of the signed inner products between the regression vectors (Drake & Klingenberg, 2008; Klingenberg & Marugán-Lobón, 2013). The analysis was performed for each individual species using MorphoJ 1.05a (Klingenberg, 2011).

For each species we included Procrustes distance (PD) and centroid size (CS) data. The PD was calculated as the square root of the sum of the squared distances between each landmark of one specimen and the mean configuration of the J1 class, and it was used as an index of shape change (e.g. Tanner *et al*., 2010; Segura & Prevosti, 2012). Centroid size was calculated as the square root of the sum of squared distances of each landmark from the centroid of the landmark configuration, and was used as an estimate of skull size (Bookstein, 1991; Zelditch *et al*., 2004). These estimations were calculated with the software R 2.9.2 (R Development Core Team, 2004), and were used to ascertain at which age class the adult skull size (CS) and adult shape (PD) were reached. We tested the differences between successive age classes using the Mann–Whitney *U*-test (Zar, 1999).

Previous studies have suggested the existence of sexual size dimorphism for these species (Gay & Best, 1995; Oliveira, 1998; Marker & Dickman, 2003); therefore, we tested for such a condition in our sample. In the case of allometric variation, both males and females clearly exhibited the same ontogenetic trajectory, with non-significant slope or intercept differences in the regression analyses, indicating that the observed allometric pattern is not biased by sexual size dimorphism. Thus, we pooled both males and females in the sample. We also tested for the presence of sexual size dimorphism in the skull, estimated as CS, and sexual shape dimorphism, estimated as PD (see Table S1), using the Mann–Whitney *U*-test (Zar, 1999), performed with the software PAST 1.98 (Hammer, Harper & Ryan, 2001).

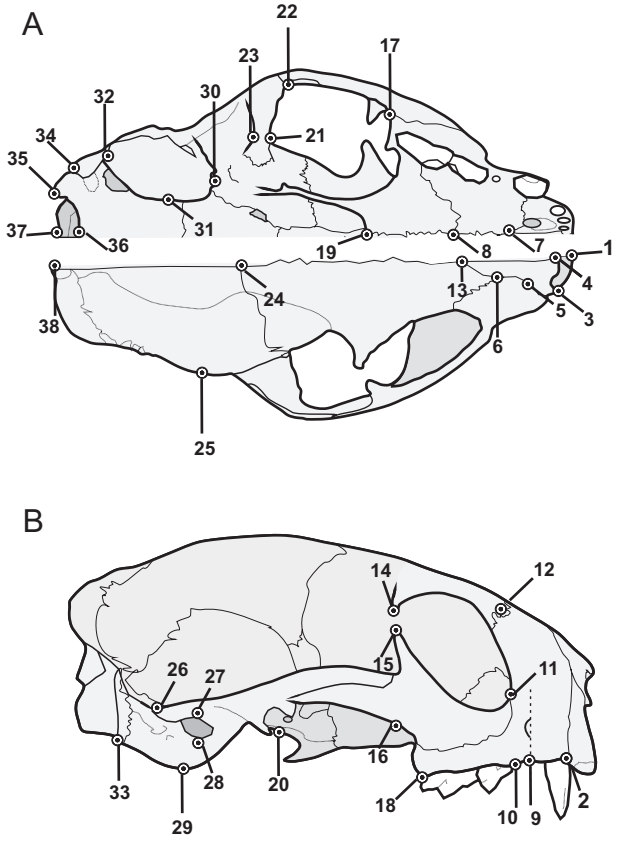

Figure 1. *Herpailurus yagouaroundi* CML 6287, illustrating 38 cranial landmarks for ventral and dorsal (A), and lateral (B) views. For key, see Table 2.

RESULTS

We found that PC1 explained 45.88% of the total variation (Fig. 2A, B), and comprised a suite of transformations towards negative values (where *A. jubatus* and *P. concolor* lie) that resulted in rounded skulls,

Figure 2. A, plot of the results of principal components 1 and 2 for the three species. B, plot of the results of principal components 1 and 3 for the three species. Circles represent *Acinonyx jubatus* specimens, squares represent *Puma concolor* specimens, and triangles represent *Herpailurus yagouaroundi* specimens. Colour key for symbols: grey, juvenile categories; white, adult categories.

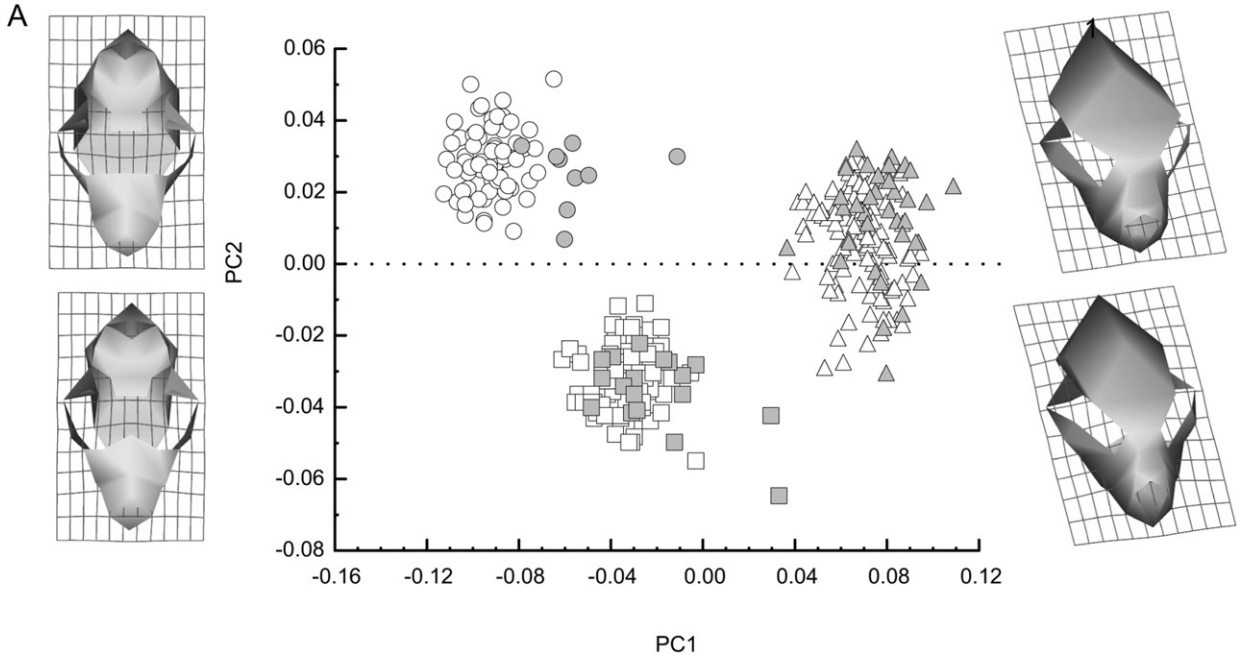
A
PC2
PC1
0.06
0.04
0.02
0.00
-0.02
-0.04
-0.06
-0.08
-0.16
-0.12
-0.08
-0.04
0.00
0.04
0.08
0.12

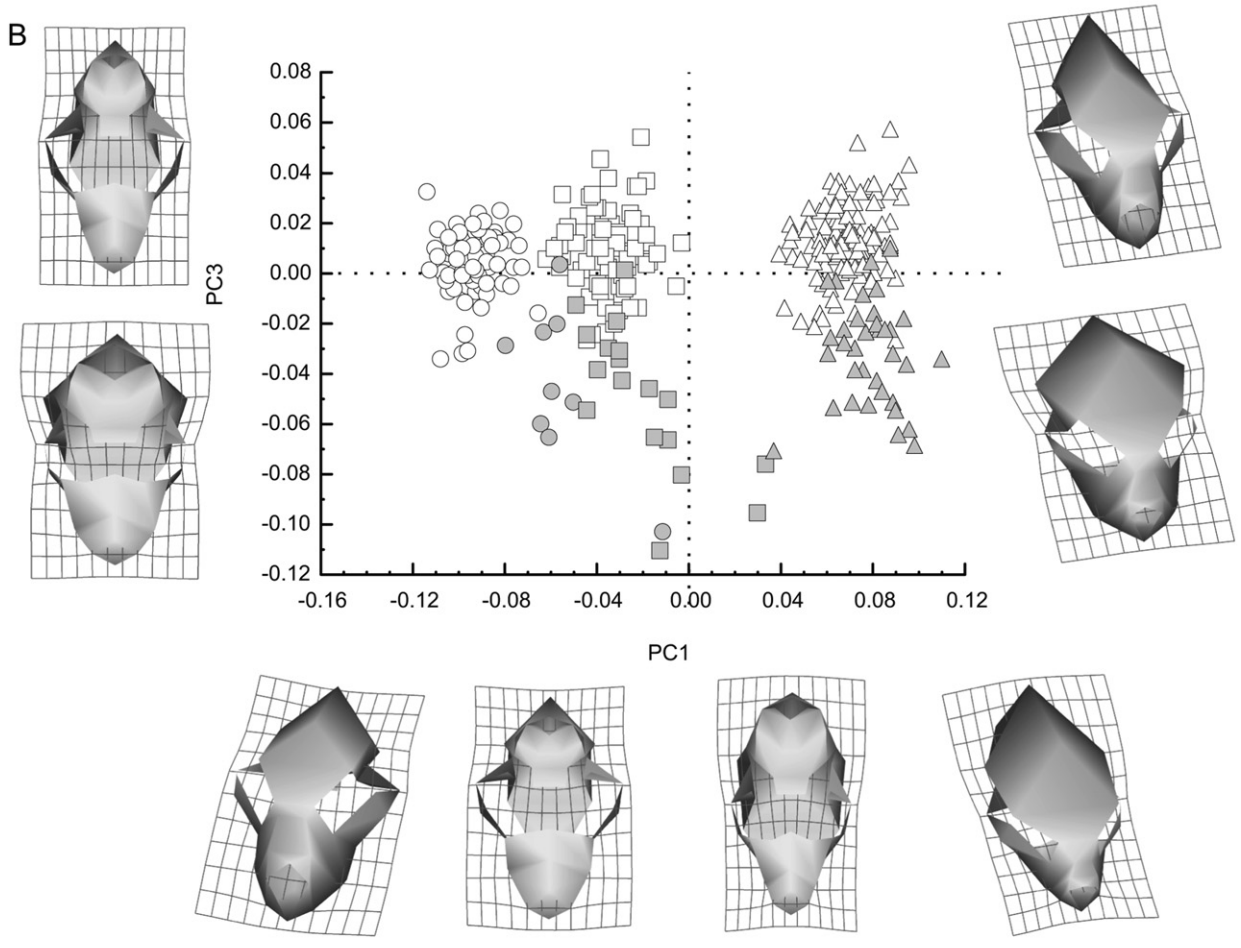
B
PC3
PC1
0.08
0.06
0.04
0.02
0.00
-0.02
-0.04
-0.06
-0.08
-0.10
-0.12
-0.16
-0.12
-0.08
-0.04
0.00
0.04
0.08
0.12

Figure 3. A, individual analysis of multivariate regression of the Procrustes coordinates against the log-transformed centroid size for *Puma concolor*. B, individual analysis of multivariate regression of the Procrustes coordinates against the log-transformed centroid size for *Herpailurus yagouaroundi*. C, individual analysis of multivariate regression of the Procrustes coordinates against the log-transformed centroid size for *Acinonyx jubatus*. Colour key for symbols: grey, juvenile categories; white, adult categories.

with short and wide face and palate, expanded zygomatic arches, relatively dorsal nasal openings and orbits, and a high muzzle. In addition, the position of the foramen magnum and the muzzle were almost ventral, with a flexion in the middle of the skull. Towards positive values (*H. yagouaroundi*), the skulls presented an enlarged braincase and basicranial region, with narrow and large palate, retracted zygomatic arches, nasal aperture and orbits in a more frontal position, and a low muzzle; the foramen magnum acquired a posterior position.

PC2 summarized 6.56% of the explained variation (Fig. 2A), and showed toward negative values (where *P. concolor* was located) enlarged and lower high braincase and muzzle, with short and wide basicranial region and palate, expanded zygomatic arches, and orbits with more dorsal position. Towards positive values (*A. jubatus*), the skulls presented a wider, domed braincase, short and tall muzzle, narrow and large basicranium and palate, and more frontally oriented orbits and maxilla.

The PC3 was associated with 5.89% of the explained variation (Fig. 2B), and variation along this axis included transformations that grouped the juvenile specimens of the three species towards negative values, characterized by rounded skulls, high braincase, broad and short muzzle and palate, foramen magnum with a more ventral position, and non-expanded zygomatic arches. Towards positive values, occupied by the adult specimens, the opposite features were observed.

Allometric variation in shape associated with size is represented in Figure 3A–C. In the individual analyses (Fig. 3A) of *P. concolor*, size explained 17.68% of shape variation ($P < 0.0001$). The larger forms presented a narrower posterior tip of the nasals, wider braincase, larger dentary row, and inion more developed towards the posterior region. Smaller forms had a wider muzzle and the orbits less close to each other. For *H. yagouaroundi* (Fig. 3B), scaling explained 7.81% of the shape variation ($P < 0.0001$), and showed, for the larger forms, more elongated rostral and basicranial region, shorter nasals, and narrower temporal fossa. Smaller specimens presented a taller braincase and larger muzzle. In the case of *A. jubatus* (Fig. 3C), size explained 13.15% of the shape variation ($P < 0.0001$). In this species, the larger forms exhibited a narrower and shorter basicranial region and wider nasals, whereas the smaller forms had orbits closer to each other, and a more vertical and straight rostral region. The shape changes associated with size are similar between *P. concolor* and *A. jubatus* (the angle between the two regression vectors was 36.20°; $P < 0.0001$). Conversely, *H. yagouaroundi* showed divergent shape changes associated with size (orthogonal regression vectors) in relation to *P. concolor* (99.72°; $P < 0.9543$) and *A. jubatus* (105.94°; $P < 0.9973$). The results showed that *H. yagouaroundi* followed a trajectory that differed from that of *P. concolor* and *A. jubatus* because the allometric shape of the skulls of *H. yagouaroundi* are clearly different in relation to size, and showed less variation than was observed in *P. concolor* and *A. jubatus*. *Puma concolor* and *A. jubatus* were very similar in size, although they were slightly different in shape. The juvenile skulls of the three species were clearly differentiated from the adult skulls.

The Mann–Whitney *U*-test showed significant differences in size and shape between age classes for *P. concolor* and *H. yagouaroundi*. In *P. concolor* these differences in CS and PD were only significant between A1 and A2. In *H. yagouaroundi*, differences in CS were found between J2 and J3, between J3 and J4, and between J4 and A1, whereas differences in PD were only found between J3 and J4 (see Table 3).

The PD for *P. concolor* (see Table 3) showed important differences between the B and J1 classes; subsequently, values were similar among juveniles and adults, and shape reached an asymptote at the J4 class (Fig. 4A). The same trend was observed for *H. yagouaroundi* (Fig. 4B), whereas *A. jubatus* showed a rapid increase in PD, to reach adult shape in class A1 (Fig. 4C).

When the sample was analyzed without taking into account the sex of the specimens (see Table 3), *P. concolor* showed a big step in CS between classes B and J1, and subsequently a constant increase from J1 to A2, at which point adult size was reached (Fig. 5A). In *H. yagouaroundi*, CS increased gradually, showing an asymptote of adult size at the A1 stage (Fig. 5B). *Acinonyx jubatus* showed rapid and sustained growth from J1 to J4, and then a step to the A1 class, at which point adult size was reached (Fig. 5C). When sex of the individuals was taken into account (Fig. S1; Table S1), a difference in CS between sexed A1, A2, and A3 was observed for the three species, changing the class in which the adult size is reached. In *P. concolor*, adult size was reached at the A1 age class, earlier than in the

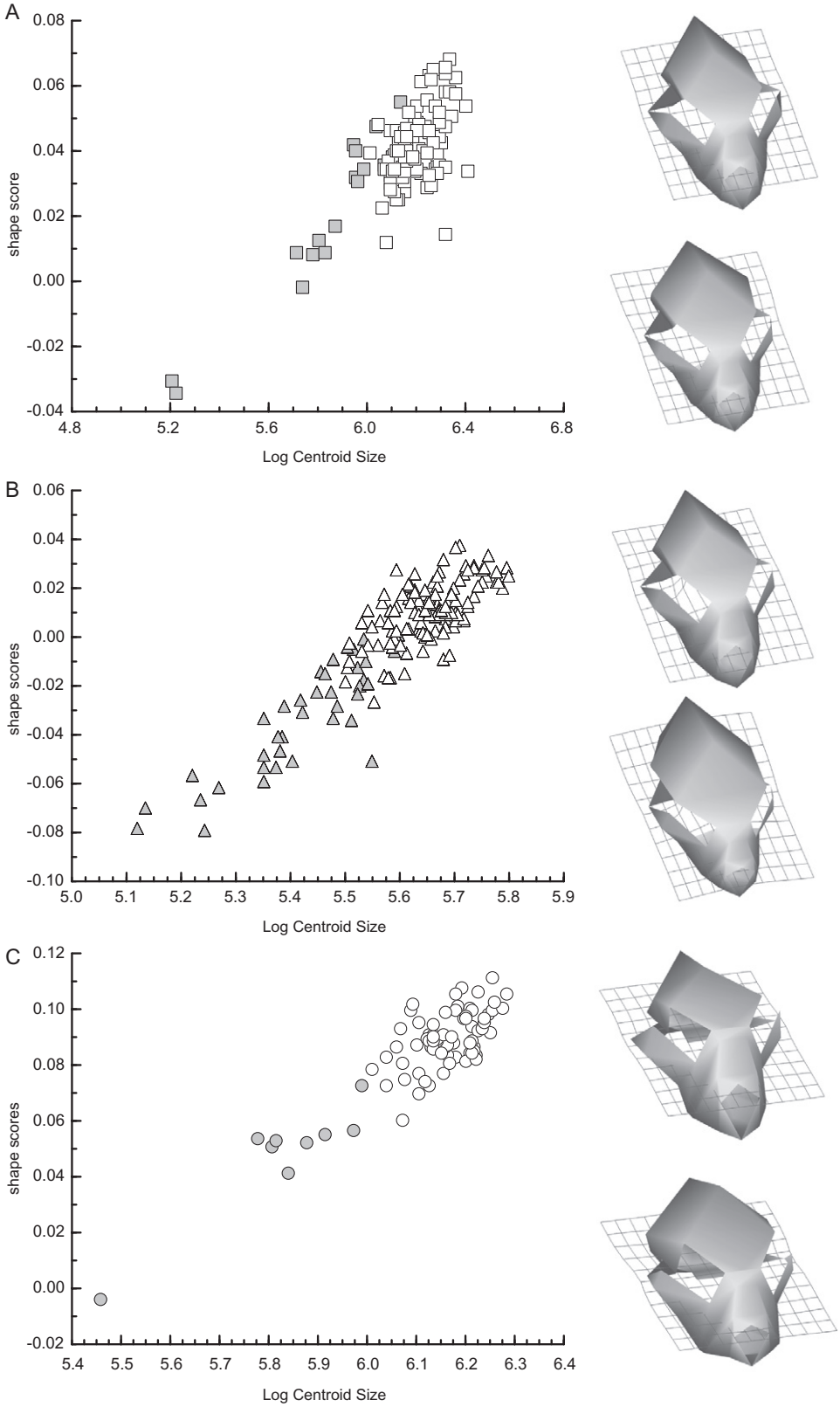
A
shape score
Log Centroid Size
B
shape scores
Log Centroid Size
C
shape scores
Log Centroid Size

Table 3. Summary of results of Mann–Whitney *U*-test between age classes for cranial allometry of *Puma concolor*, *Herpailurus yagouaroundi*, and *Acinonyx jubatus*

	U	*n1*	*n2*	*P*
Centroid size (CS)				
Puma concolor				
A1–A2	**473.0000**	**37**	**39**	**0.009809**
A2–A3	308.0000	39	16	0.940911
Herpailurus yagouaroundi				
J1–J2	15.00000	11	5	0.156746
J2–J3	**4.000000**	**5**	**11**	**0.007762**
J3–J4	**12.00000**	**11**	**7**	**0.016395**
J4–A1	**54.00000**	**7**	**53**	**0.002461**
A1–A2	1040.000	53	48	0.114639
A2–A3	239.0000	48	12	0.365177
Acinonyx jubatus				
A1–A2	483.0000	34	33	0.327969
Procrustes distance (PD)				
Puma concolor				
A1–A2	**498.0000**	**37**	**39**	**0.020197**
A2–A3	233.0000	39	16	0.143204
Herpailurus yagouaroundi				
J1–J2	14.00000	11	5	0.126168
J2–J3	23.00000	5	11	0.610194
J3–J4	**9.000000**	**11**	**7**	**0.007547**
J4–A1	184.0000	7	53	0.972446
A1–A2	1258.000	53	48	0.924152
A2–A3	278.0000	48	12	0.853382
Acinonyx jubatus				
A1–A2	452.0000	34	33	0.171629

Comparisons with *P*-values significant at 0.05 level are set in bold.

case of the pooled sample, although it is not clear whether adult size occurred in a previous stage because of the absence of males in the J3 class, and the absence of males and females in the J4 class in our sample. In *H. yagouaroundi* adult size was reached at the J4 age stage, earlier than in the pooled sample (as in *P. concolor*); however, in J4 we did not detect differences in skull size between males and females. The difference between sexes started at the A1 class, and it was observed in all adult age stages. As in *P. concolor*, adult males of *H. yagouaroundi* were larger than the females, and the females reached the asymptote at lower CS values than in the males. In *A. jubatus* the difference was more visible between adult classes from A1 to A3, with males looking slightly larger than the females. Adult size was reached at the A1 age stage, the same as in the pooled sample.

DISCUSSION

Skull ontogeny in the Puma lineage

The idea that felids have conservative skulls, if compared with other carnivore families, is frequently found in the literature, and is generally accepted (Goswami, 2006; Christiansen, 2008; Sunquist & Sunquist, 2009). However, in an analysis with a lower taxonomic level (in this lineage), the results showed that the skulls of these three highly related species exhibited conspicuous differences during ontogeny (Fig. 2A, B).

The three species occupy different locations in morphospace. In this sense, *A. jubatus* and *P. concolor* showed shorter and wider skulls, with more expanded zygomatic arches, than *H. yagouaroundi*, which exhibited a narrow and elongated braincase and basicranium, and non-expanded zygomatic arches (Fig. 2A, B). In addition, angular comparisons showed that *H. yagouaroundi* presented the most divergent pattern of change in its ontogenetic trajectory, relative to the other two species, showing a greater variation in the skull, and also being the smallest species in this clade (Figs 2A, B, 3B). This fact suggests that the evolution of the group did not give rise to a smaller, morphologically similar version of a larger predator in *H. yagouaroundi* (i.e. it does not represent a scaled skull of *A. jubatus* or *P. concolor*). The clear

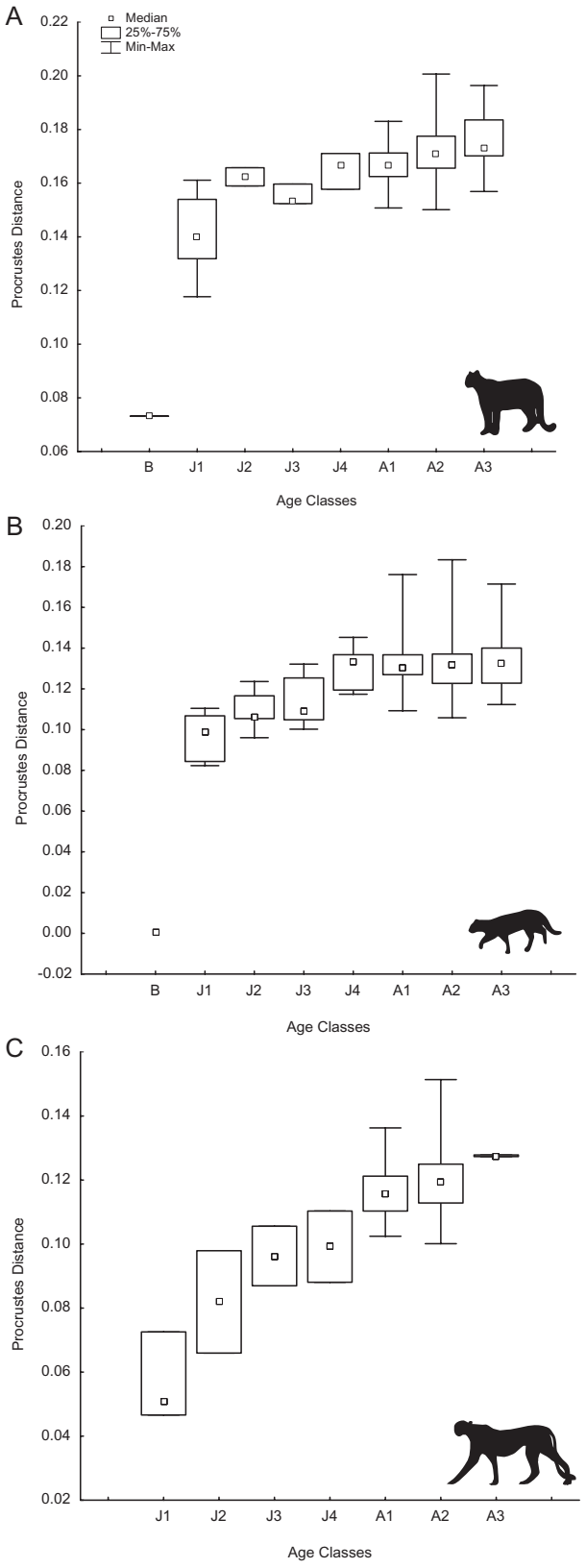

Figure 4. Box plots of cranial procrustes distance of each specimen of all age classes to the mean for: (A) *Puma concolor*; (B) *Herpailurus yagouaroundi*; and (C) *Acinonyx jubatus*. The box plots include median, upper, and lower quartiles (75 and 25%, respectively), and minima and maxima.

separation between juvenile and adult skull morphology was supported by differences in the braincase, rostrum, and zygomatic arches (Fig. 2B). However, it is worth noting that the different adult classes were not differentiated along any of the PCs analysed, indicating that the reported stabilization in shape change occurs earlier in ontogeny, during the juvenile stages (*P. concolor* and *H. yagouaroundi*), or in the first adult ontogenetic phase (*A. jubatus*) (Fig. 4A–C). Therefore, large intraspecific shape differences between the skulls of different adult age classes clearly are not present on either PCA or PD (except for *P. concolor*; Table 3). Although both juvenile and adult skulls of the three species showed differences during ontogeny (Fig. 2B), the juveniles of *P. concolor* and *A. jubatus* had similar CS values as the adults of *H. yagouaroundi* (Fig. 3A, B).

Although previous works have indicated that phylogeny strongly influences skull shape (e.g. Goswami, 2006; Wroe & Milne, 2007; Figueirido *et al*., 2011), in this work we cannot apply phylogenetic comparative methods, and so we cannot either refute or support this hypothesis. Our results suggest that there are greater morphological similarities between *P. concolor* and *A. jubatus* than between *P. concolor* and *H. yagouaroundi*, as would be expected according to phylogeny. Therefore, the evolution of the ontogenetic change in the Puma lineage seems to be more influenced by size. This finding was previously observed by Sicuro & Oliveira (2010) and Sicuro (2011), who analysed the skull structure of adult specimens. According to Morales & Giannini (2010) and Sicuro (2011), in closely related and sympatric species (such as *P. concolor* and *H. yagouaroundi*), size differentiation is probably related to mechanisms that reduce niche overlap and/or interspecific competition, such as character displacement and size assortment.

With the life-history information we have to hand (see Material and methods), we know that *P. concolor* and *A. jubatus* are born bigger and have longer gestational periods than *H. yagouaroundi*: i.e. fetuses of *P. concolor* and *A. jubatus* grow over a longer period. It is highly probable that the ancestor of this group was large in size, a condition maintained for *A. jubatus* and *P. concolor*. As *A. jubatus* is basal with respect to the clade *P. concolor–H. yagouaroundi*, we could

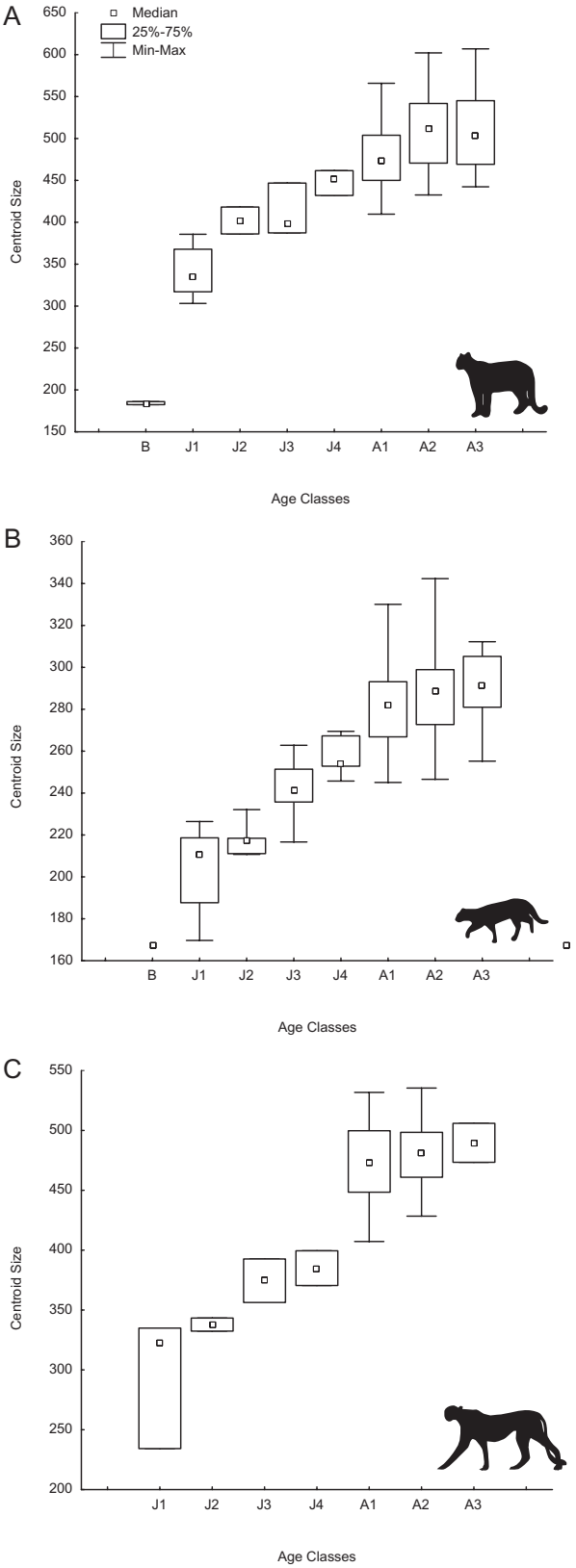

Figure 5. Box plots of skull centroid size versus age classes for: (A) *Puma concolor*; (B) *Herpailurus yagouaroundi*; and (C) *Acinonyx jubatus*. The box plots include median, upper, and lower quartiles (75 and 25%, respectively), and minima and maxima.

hypothesize that *H. yagouaroundi* is paedomorphic. This type of heterochrony could be produced by a more delayed onset of growth (post displacement), an earlier offset (progenesis or hypomorphosis), or by a reduced rate of growth (neoteny or deceleration) (Reilly, Wiley & Meinhardt, 1997; Klingenberg, 1998; McNamara, 2012); however, this must be tested in a more inclusive cladistic context. Phylogeny seems to influence the timing of reaching the final skull shape during ontogeny. The closely related *P. concolor* and *H. yagouaroundi* reach their definitive shape earlier (J4 class) than *A. jubatus* (A1 class, i.e. when permanent dentition is fully erupted) (Fig. 4A–C). In this sense, both closely related species achieved their optimal performance (in relation to predatory behaviour) at the same ontogenetic stage, although they arrived at a different final skull shape and size. On the other hand, *A. jubatus* reached adult shape and size simultaneously (in A1 class), whereas *P. concolor and H. yagouaroundi* attained adult shape before adult size (in J4 class) (Figs 4A–C, 5A–C).

Adults of *A. jubatus* showed a characteristic dome formed by extensive frontal sinuses, which alleviate the high oxygen demand produced by high-speed chases (Salles, 1992; Marker & Dickman, 2003; Torregrosa *et al*., 2010) (Fig. 2A). This vaulted braincase was not observed in other felids of the group. In addition, *P. concolor* exhibited a narrower postorbital constriction and larger temporal fossa compared with *A. jubatus* (Fig. 2A). Such results are in agreement with the suggestion of clustering *P. concolor* with the pantherines, on the basis of the robustness of the adult skull, whereas *A. jubatus* was noted to be closest structurally to the small cats (Meachen-Samuels & Van Valkenburgh, 2009). However, our results indicate that the configuration of both *A. jubatus* and *P. concolor* was more favourable for mechanical advantage than that of *H. yagouaroundi*, in terms of reduced out-lever lengths as well as an increased area for the attachment of masticatory musculature (Radinsky, 1981; Wroe & Milne, 2007; Prevosti *et al*., 2010) (Fig. 2A). Among big cats, *P. concolor* exhibited a narrower postorbital constriction and larger temporal fossa than *A. jubatus*, providing a larger area for the origin of the temporalis muscle, and thus indicating its increased mechanical performance (Prevosti *et al*., 2010; Sicuro & Oliveira,

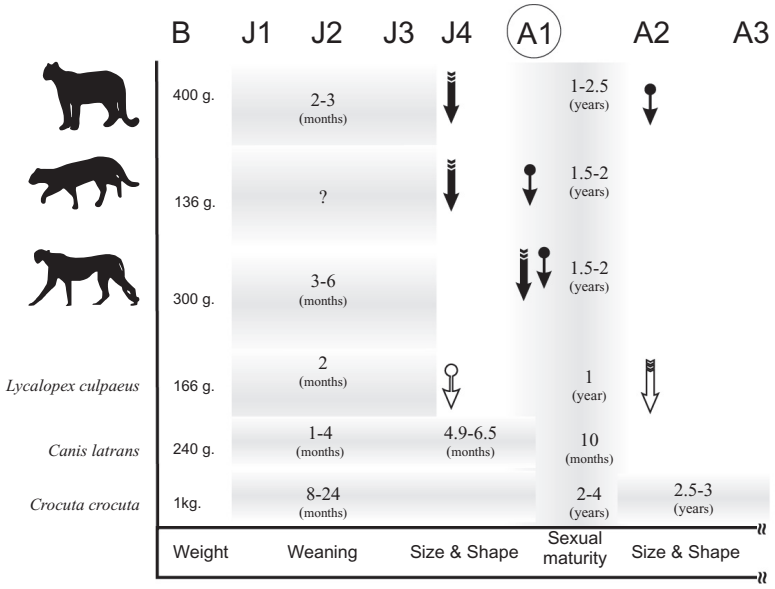

Figure 6. Timeline illustrating the age classes in relation to life-history events taken from literature to (*Puma concolor*), (*Herpailurus yagouaroundi*), (*Acinonyx jubatus*), *Lycalopex culpaeus*, *Canis latrans*, and *Crocuta crocuta*. Represents size and represents shape. Black arrows represent information from three-dimensional geometric morphometrics, and white arrows represent information from two-dimensional geometric morphometrics.

2010) (Fig. 2A). The structure of the skull in *H. yagouaroundi* completely differed from the remaining species. This was in agreement with the low accuracy for assigning *H. yagouaroundi* to this lineage (because of its disparate morphotype) when a phylomorphospace analysis was performed, whereas *A. jubatus* and *P. concolor* were easily assigned (Sakamoto & Ruta, 2012).

Our results indicate that shape changes (from J1 to adult shape) were greater (higher PD values) in *P. concolor* and *H. yagouaroundi* than in *A. jubatus* (Fig. 4A–C), and these changes were completed in less time, before sexual maturity in *P. concolor* and *H. yagouaroundi*, and at sexual maturity in *A. jubatus* (Fig. 6). Thus, the rate of shape change is higher in the first two species. Size showed a slightly different pattern because *H. yagouaroundi* (Fig. 5B) presented the highest rate of change (with a greater difference between J1 and adult CS values) and shortest time of development (until sexual maturity, Fig. 6), whereas *P. concolor* presented less change in CS (Fig. 5A) but a longer period of development (after sexual maturity, Fig. 6). *Acinonyx jubatus* showed the least change in CS (Fig. 5C), but its period of development was shorter than in *P. concolor* (until sexual maturity, Fig. 6), thus its rate of size change could be higher or similar to the latter felid. These results indicate that absolute size and shape change are not correlated with time of development; therefore, some species could attain great changes in less time than others. The ontogenetic allometry (shape against size) also indicates the presence of some differences (Fig. 3), because *P. concolor* and *A. jubatus* have a similar trend, whereas *H. yagouaroundi* presents a higher intercept (larger shape score at lowest CS) and a shorter trajectory because of its small adult size (Fig. 3). However, the final shape score from allometry is similar in the three species. The similarity between the first two species could be explained by their similar size range during ontogeny, contrasting with the smaller range of *H. yagouaroundi*, a constraint that has been detected for adult skulls in Felidae (see Morales & Giannini, 2010; Sicuro, 2011; see above). More data on skull ontogeny of other felids are needed to corroborate that these similarities are the result of size constraints.

Functional interpretations

Changes observed between juvenile and adult skulls (Fig. 2B) were in general related to the enhancement of predatory skills, in agreement with dietary changes from milk to carnivory, mainly in the larger species. The enlargement of the temporal fossa, as a result of the narrower braincase and expanded zygomatic arches in adults, provides a space for the massive attachment of the temporal and masseteric muscles (Fig. 2B). These changes followed the same pattern of positive allometry of the facial skeleton and negative allometry of the neurocranium previously observed

for felids (Segura & Flores, 2009; Slater & Van Valkenburgh, 2009; Giannini *et al*., 2010; Prevosti *et al*., 2010). Several authors have provided additional approaches to account for shape changes during the evolution of ontogeny, pointing to diet (e.g. Radinsky, 1981; Sunquist & Sunquist, 2002; Wroe & Milne, 2007) because it is related to the functional integration of traits involved in mastication (see Goswami, 2006). Although the three species studied here have the same diet (hypercarnivorous), they hunt prey of different sizes. *Puma concolor* has an extensive range of prey (reflecting its wider geographic distribution), from agoutis and armadillos to deer and guanacos. *Herpailurus yagouaroundi* feeds primarily on small vertebrates weighing less than 1 kg, such as birds and medium-sized rodents. Finally, *A. jubatus* is highly specialized to prey on gazelles and small to medium-sized antelopes (Sunquist & Sunquist, 2009).

Comparison with other carnivores

Although we detected different patterns of change during ontogeny in the three species, suggesting that the skull is not conservative in the Puma lineage, these ontogenetic patterns contrast with other carnivorans with completely different hunting and biting strategies, such as canids and hyaenids. For instance, the fact that *P. concolor* and *H. yagouaroundi* reached their final skull shape before reaching their final size and sexual maturity is a different pattern that contrasts with that of canids such as *Lycalopex culpaeus* (Fig. 6), in which adult size is reached before sexual maturity, and adult shape is only reached after this biological event (around 7 months for adult size and over 1 year for adult shape; Segura & Prevosti, 2012). In the case of *Canis latrans* (La Croix *et al*., 2011a, b), both adult shape and size were reached between 4.9 and 6.5 months old, which is equivalent to the juvenile classes in our sample, i.e. before sexual maturity (Fig. 6). On the other hand, the hyaenid *Crocuta crocuta* (Tanner *et al*., 2010) reaches its adult size at 29 months and adult shape at 35 months, near or during sexual maturity (24–48 months; Holekamp & Kolowski, 2009) (Fig. 6). This retardation in development and growth is linked to their delayed weaning (8–24 months old), and could be related to the high specialization of hyaenids for durophagy (La Croix *et al*., 2011a). Unfortunately, it was not possible to homologate the absolute ages of *Canis latrans* and *Crocuta crocuta* with the age stages in our sample (Fig. 6). However, the general pattern of ontogenetic change found in the Puma lineage, and reported here, appears to be directed towards strengthening the skull in relation to the adult's shift to a carnivorous diet. A similar trend was previously detected in species studied with different methods (e.g. *P. concolor*, Segura & Flores, 2009; Giannini *et al*., 2010; *Lycalopex culpaeus*, Segura & Prevosti, 2012; Segura, 2013; *Canis latrans*, La Croix *et al*., 2011a, b; *Crocuta crocuta*, Tanner *et al*., 2010). Using sexual maturity as a landmark to compare these species (Fig. 6), other patterns are difficult to explain. For example, the delayed attainment of adult skull shape in *Lycalopex culpaeus*, which could be explained by ecological and behavioural factors (see Segura & Prevosti, 2012), does not occur in the other canid studied (*Canis latrans*), or even in in hypercarnivorous species such as the felids studied here or *Crocuta crocuta*. This could be an artifact created by the lack of precise timing of size and morphological changes, and for other biological events (e.g. the end of parental care).

Although the patterns detected in these species have a common component (i.e. skull strengthening along ontogeny), the skull differences in previously studied groups, such as canids and hyaenids, suggest the existence of alternative strategies in the growth and development of carnivores. For instance, some canids, such as *Canis latrans* (La Croix *et al*., 2011a, b) and *Lycalopex culpaeus* (Segura & Prevosti, 2012), present a growth pattern similar to that of large felids, such as *P. concolor* and *A. jubatus* (i.e. well-developed sagittal and occipital crests, and a narrowing of the braincase). However, the extreme reinforcement of the bite mechanism seen in hyaenids (i.e. massive braincase and zygomatic arches, and a large sagittal crest; La Croix *et al*., 2011a) was not detected in the Puma lineage. Similarly, rostrum elongation seems to be a generalized characteristic observed in canids (Wayne, 1986; Drake, 2011; La Croix *et al*., 2011a, b; but see Segura & Prevosti, 2012), but is absent in felids. According to Sears *et al*. (2007) and Pointer *et al*. (2012), a transcription factor (Runx2) is involved in osteoblast differentiation, being a candidate for regulating heterochronic changes in the facial morphology of carnivores. For instance, its down-regulation would result in the earlier truncation of facial bone development (i.e. progenesis/hypomorphosis), but if it is up-regulated development would be extended (i.e. hypermorphosis). In relation to the muzzle, the allometric change during ontogeny in felids is minimal, for which the skull in this group seems to be conservative in comparison with other carnivorans (Wayne, 1986; Sears *et al*., 2007; McNamara, 2012).

Further studies should focus on the knowledge of cranial ontogeny in related felids, and their natural history and growth, in order to relate the respective growth patterns with ontogeny and behaviour. It would also be highly interesting to test these hypotheses in a strict phylogenetic context, in order to obtain a more robust reconstruction of skull evolution in this group.

ACKNOWLEDGEMENTS

For the permission and attention in the study of the material under their care we thank Kristofer Helgen and Darrin Lunde (National Museum of Natural History, Smithsonian Institution), Bruce Patterson and Bill Stanley (Field Museum of Natural History), Robert Voss and Eileen Westwig (American Museum of Natural History), Sergio Bogan and Yolanda Davies (Colección Félix de Azara), Rubén Barquez and Mónica Díaz (Colección Mamíferos Lillo), David Flores and Sergio Lucero (Museo Argentino de Ciencias Naturales Bernardino Rivadavia), and Diego Verzi and Itatí Olivares (Museo de La Plata). We also wish to thank David Flores, who discussed an earlier version of this article, Gregory Breton, who shared information about *Herpailurus yagouaroundi*, and Cecilia Morgan, for her revision of the English grammar. We also thank Lars Werdelin and an anonymous reviewer who provided precise comments that considerably improved this article. This research was partially supported by a Short Term Visitor Fellowship Award from The National Museum of Natural History, Smithsonian Institution (NMNH), and a Visiting Scholarship Award from The Field Museum of Natural History (FMNH). This is a contribution to the Projects PICT 2008-1798 and 2011-0309 of the Agencia Nacional de Promoción Científica y Tecnológica (ANPCyT) and PIP 112-201101-00164 of CONICET.

REFERENCES

Barnett R, Barnes I, Phillips MJ, Martin LD, Harington CR, Leonard JA, Cooper A. 2005. Evolution of the extinct Sabertooths and the American Cheetahlike cat. *Current Biology* **15:** R589–R590.

Bininda-Emonds ORP, Gittleman JL, Purvis A. 1999. Building large trees by combining phylogenetic information: a complete phylogeny of the extant Carnivora (Mammalia). *Biological Review* **74:** 143–175.

Bookstein FL. 1991. *Morphometric tools for landmark data. Geometry and biology*. New York: Cambridge University Press.

Breton G. 2007. European Studbook for the Jaguarundi (*Herpailurus yaguarondi*). *Le Parc des Félins & EAZA Report* 1–67.

Broom R. 1949. Notes on the milk dentition of the lion, leopard and cheetah. *Annals Transvaal Museum* **21:** 183–185.

Buzas B, Gulyas E. 2012. Hand-raising Jaguarundis (*Puma yagouaroundi*). *Feline Conservation Federation* **56:** 1–4.

Caro TM. 1994. *Cheetahs of the Serengeti Plains: group living in an asocial species*. Chicago, IL: University of Chicago Press.

Cassini GH, Vizcaíno SF. 2012. An approach to the biomechanics of the masticatory apparatus of early miocene (Santacrucian age) South American ungulates (Astrapotheria, Litopterna, and Notoungulata): moment arm estimation based on 3D landmarks. *Journal of Mammalian Evolution* **19:** 9–25.

Christiansen P. 2008. Evolution of skull and mandible shape in cats (Carnivora: Felidae). *PLoS ONE* **3:** e2807.

Christiansen P. 2012. The Making of a Monster: postnatal ontogenetic changes in craniomandibular shape in the great sabercat *Smilodon*. *PLoS ONE* **7:** e29699. doi:10.1371/journal.pone.0029699.

Christiansen P, Mazák JH. 2009. A primitive Late Pliocene cheetah and evolution of the cheetah lineage. *PNAS* **106:** 512–515.

Crowe DM. 1975. Aspects of ageing, growth, and reproduction of bobcats from Wyoming. *Journal of Mammalogy* **56:** 177–198.

Currier MJP. 1983. *Felis concolor*. *Mammalian Species* **200:** 1–7.

Drake AG. 2011. Dispelling dog dogma: an investigation of heterochrony in dogs using 3D geometric morphometric analysis of skull shape. *Evolution and Development* **13:** 204–213.

Drake AG, Klingenberg CP. 2008. The pace of morphological change: historical transformation of skull shape in St Bernard dogs. *Proceedings of the Royal Society* **275:** 71–76.

Drake AG, Klingenberg CP. 2010. Large-scale diversification of skull shape in domestic dogs: disparity and modularity. *The American Naturalist* **175:** 289–301.

Dryden IL, Mardia KV. 1998. *Statistical shape analysis*. Chichester: Wiley.

Eaton RL, Verlander KA. 1977. Reproduction in the puma: biology, behavior and ontogeny. In: Eaton RL, ed. *The world's cats*. Seattle, WA: Carnivore Research Institute, Burke Museum, 45–70.

Fagen RM, Wiley KS. 1978. Felid paedomorphosis, with special reference to *Leopardus*. *Carnivore* **1:** 72–81.

Figueirido B, MacLeod N, Krieger J, De Renzi M, Pérez-Claros JA, Palmqvist P. 2011. Constraint and adaptation in the evolution of carnivoran skull shape. *Paleobiology* **37:** 490–518.

Figueirido B, Serrano-Alarcón FJ, Slater GJ, Palmqvist P. 2010. Shape at the cross-roads: homoplasy and history in the evolution of the carnivoran skull towards herbivory. *Journal of Evolutionary Biology* **23:** 2579–2594.

Figueirido B, Soibelzon LH. 2010. Inferring paleoecology in extinct tremarctine bears using geometric morphometries. *Lethaia* **43:** 209–232.

Figueirido B, Tseng ZJ, Martín-Serra A. 2013. Skull shape evolution in duropahgous carnivorans. *Evolution* **67:** 1975–1993.

García-Perea R. 1996. Patterns of postnatal development in skulls of lynxes, Genus *Lynx* (Mammalia: Carnivora). *Journal of Morphology* **229:** 241–254.

Gay SW, Best TL. 1995. Geographic variation in sexual dimorphism of the puma (*Puma concolor*) in North and South America. *The Southwestern Naturalist* **40:** 148–159.

Gay SW, Best TL. 1996. Age-related variation in skulls of the puma (*Puma concolor*). *Journal of Mammalogy* **77:** 191–198.

Giannini NP, Segura V, Giannini MI, Flores D. 2010. A quantitative approach to the cranial ontogeny of the puma. *Mammalian Biology* **75:** 547–554.

Goodall C. 1991. Procrustes methods in the statistical analysis of shape. *Journal of the Royal Statistical Society* **53:** 285–339.

Goswami A. 2006. Morphological integration in the carnivoran skull. *Evolution* **60:** 169–183.

Goswami A, Milne N, Wroe S. 2011. Biting through constraints: cranial morphology, disparity and convergence across living and fossil carnivorous mammals. *Proceedings of the Royal Society* **278:** 1831–1839.

Hammer Ø, Harper DAT, Ryan PD. 2001. PAST: paleontological statistics software package for education and data analysis. *Palaeontologia Electronica* **4:** 1–9. Available at: http://palaeo-electronica.org/2001_1/past/past.pdf

Holekamp KE, Kolowski JM. 2009. Family Hyaenidae (Hyaenas). In: Wilson DE, Mittermeier RA, eds. *Handbook of the mammals of the world 1 carnivores*. Barcelona: Lynx Editions, 234–260.

Holliday JA, Steppan SJ. 2004. Evolution of hypercarnivory: the effect of specialization on morphological and taxonomic diversity. *Paleobiology* **30:** 108–128.

Johnson WE, Eizirik E, Pecon-Slattery J, Murphy WJ, Antunes A, Teeling E, O'Brien SJ. 2006. The Late Miocene radiation of modern Felidae: a genetic assessment. *Science* **311:** 73–77.

Johnson WE, O'Brien SJ. 1997. Phylogenetic Reconstruction of the Felidae using 16S rRNA and NADH-5 mitochondrial genes. *Journal of Molecular Evolution* **44:** S98–S116.

Kitchener A. 1991. *The natural history of the wild cats*. New York: Comstock Publishing Associates.

Klingenberg CP. 1998. Heterochrony and allometry: the analysis of evolutionary change in ontogeny. *Biological Reviews* **73:** 79–123.

Klingenberg CP. 2011. MorphoJ: an integrated software package for geometric morphometrics. *Molecular Ecology Resources* **11:** 353–357.

Klingenberg CP, Marugán-Lobón J. 2013. Evolutionary covariation in geometric morphometric data: analyzing integration, modularity and allometry in a phylogenetic context. *Systematic Biology*. doi: 10.1093/sysbio/syt025.

Krausman PR, Morales SM. 2005. *Acinonyx jubatus*. *Mammalian Species* **771:** 1–6.

La Croix S, Holekamp KE, Shivik JA, Lundrigan BL, Zelditch ML. 2011a. Ontogenetic relationships between cranium and mandible in coyotes and hyenas. *Journal of Morphology* **272:** 662–674.

La Croix S, Zelditch ML, Shivik JA, Lundrigan BL, Holekamp KE. 2011b. Ontogeny of feeding performance and biomechanics in coyotes. *Journal of Zoology* **285:** 301–315.

Marker LL, Dickman AJ. 2003. Morphology, physical condition, and growth of the cheetah (*Acinonyx jubatus jubatus*). *Journal of Mammalogy* **84:** 840–850.

Mattern MY, McLennan DA. 2000. Phylogeny and speciation of Felids. *Cladistics* **16:** 232–253.

Mazák V. 1981. *Panthera tigris*. *Mammalian Species* **152:** 1–8.

McNamara KJ. 2012. Heterochrony: the evolution of development. *Evolution: Education and Outreach* **5:** 203–218.

Meachen-Samuels J, Van Valkenburgh B. 2009. Craniodental indicators of prey size preference in the Felidae. *Biological Journal of the Linnean Society* **96:** 784–799.

Meloro C, Raia P, Piras P, Barbera C, O'Higgins P. 2008. The shape of the mandibular corpus in large fissiped carnivores: allometry, function and phylogeny. *Zoological Journal of the Linnean Society* **154:** 832–845.

Mitteroecker P, Gunz P, Bernhard M, Schaefer K, Bookstein FL. 2004. Comparison of cranial ontogenetic trajectories among great apes and humans. *Journal of Human Evolution* **46:** 679–698.

Morales MM, Giannini NP. 2010. Morphofunctional patterns in Neotropical felids: species co-existence and historical assembly. *Biological Journal of the Linnean Society* **100:** 711–724.

O'Brien SJ, Johnson WE. 2007. The evolution of cats. *Scientific American* **297:** 68–75.

O'Higgins P, Jones N. 2006. *Tools for statistical shape analysis*. North Yorkshire: Hull York Medical School.

Oliveira TG. 1998. *Herpailurus yagouaroundi*. *Mammalian Species* **578:** 1–6.

Petersen MK, Petersen MK. 1978. Growth rate and other postnatal developmental changes in margays. *Carnivore* **1:** 87–92.

Pointer MA, Kamilar JM, Warmuth V, Chester SGB, Delsuc F, Mundy NI, Asher RJ, Bradley BJ. 2012. RUNX2 tandem repeats and the evolution of facial length in placental mammals. *BMC Evolutionary Biology* **12:** 1471–2148.

Prevosti FJ, Turazzini GF, Chemisquy MA. 2010. Morfología craneana en tigres dientes de sable: alometría, función y filogenia. *Ameghiniana* **47:** 239–256.

R Development Core Team. 2004. *R: a language and environment for statistical computing*. Vienna: R Foundation forStatistical Computing, Available at: http://www.rproject.org

Radinsky LB. 1981. Evolution of skull shape in carnivores. I. Representative modern carnivores. *Biological Journal of the Linnean Society* **15:** 369–388.

Reilly SM, Wiley EO, Meinhardt DJ. 1997. An integrative approach to heterochrony: the distinction between interspecific and intraspecific phenomena. *Biological Journal of the Linnean Society* **60:** 119–143.

Rohlf FJ. 1999. Shape statistics: procrustes method for the optimal superimposition of landmarks. *Systematic Zoology* **39:** 40–59.

Sakamoto M, Ruta M. 2012. Convergence and divergence in the evolution of cat skulls: temporal and spatial patterns of morphological diversity. *PLoS ONE* **7:** 1–13.

Salles LO. 1992. Felid phylogenetics: extant taxa and skull morphology (Felidae, Aeluroidea). *American Museum Novitates* **3047:** 1–67.

Sears KE, Goswami A, Flynn JJ, Niswandera LA. 2007. The correlated evolution of Runx2 tandem repeats,

transcriptional activity, and facial length in Carnivora. *Evolution & Development* **9:** 555–565.

Segura V. 2013. Skull ontogeny of Lycalopex culpaeus (Carnivora: Canidae): description of cranial traits and craniofacial sutures. *Mammalia* **77:** 205–214.

Segura V, Flores DA. 2009. Aproximación cualitativa y aspectos funcionales en la ontogenia craneana de *Puma concolor* (Felidae). *Mastozoología Neotropical* **16:** 169–182.

Segura V, Prevosti F. 2012. A quantitative approach to the cranial ontogeny of *Lycalopex culpaeus* (Carnivora: Canidae). *Zoomorphology* **131:** 79–92.

Shaw HG, Beier P, Culver M, Grigione M. 2007. *Puma field guide*. The Cougar Network.

Sicuro F. 2011. Evolutionary trends on extant cat skull morphology (Carnivora: Felidae): a three-dimensional geometrical approach. *Biological Journal of the Linnean Society* **103:** 176–190.

Sicuro F, Oliveira LFB. 2010. Skull morphology and functionality of extant felidae (mammalia: carnivora): a phylogenetic and evolutionary perspective. *Zoological Journal of the Linnean Society* **161:** 414–462.

Slater GJ, Van Valkenburgh B. 2009. Allometry and performance: the evolution of skull form and function in felids. *Journal of Evolutionary Biology* **22:** 2278–2287.

Stander PE. 1997. Field age determination of Leopards by tooth wear. *African Journal of Ecology* **35:** 156–161.

Stehlik J. 1971. Breeding jaguars *Panthera onca* at Ostrava Zoo. *International Zoo Yearbook* **11:** 116–118.

Stuart CHT, Stuart TD. 1985. Age determination and development of foetal and juvenile Felis caracal Schreber, 1776. *Säugertierkunde Mitteilungen* **32:** 217–229.

Sunquist M, Sunquist F. 2002. *Wild cats of the world*. Chicago, IL: University of Chicago press.

Sunquist M, Sunquist F. 2009. Family Felidae. In: Wilson DE, Mittermeier RA, eds. *Handbook of the mammals of the world 1 carnivores*. Barcelona: Lynx editions, 54–168.

Tanner JB, Zelditch ML, Lundrigan BL, Holekamp KE. 2010. Ontogenetic change in skull morphology and mechanical advantage in the spotted hyena (*Crocuta crocuta*). *Journal of Morphology* **271:** 353–365.

Torregrosa V, Petrucci M, Pérez-Claros JA, Palmqvist P. 2010. Nasal aperture area and body mass in felids: ecophysiological implications and paleobiological inferences. *Geobios* **43:** 653–661.

Van Valkenburgh B, Grady F, Kurtén B. 1990. The Plio-Pleistocene Cheetah-like cat *Miracinonyx inexpectatus* of North America. *Journal of Vertebrate Paleontology* **10:** 434–454.

Volf J. 1972. Exigences alimentaires et dentition des jeunes de trois especes de felides. *Mammalia* **36:** 683–686.

Wayne RK. 1986. Cranial morphology of domestic and wild canids: the influence of development on morphological change. *Evolution* **40:** 243–261.

Werdelin L, Yamaguchi N, Johnson WE, O'Brien SJ. 2010. Phylogeny and evolution of cats (Felidae). In: Macdonald DW, Loveridge AJ, eds. *Biology and conservation of wild felids*. New York: Oxford University Press, 59–82.

Wroe S, Milne N. 2007. Convergence and remarkably consistent constraint in the evolution of carnivore skull shape. *Evolution* **61:** 1251–1260.

Zar JH. 1999. *Biostatistical analysis, 4th edn*. Upper Saddle River: Prentice-Hall.

Zelditch ML, Swiderski D, Sheets H, Fink W. 2004. *Geometric morphometrics for biologists: a primer*. London: Elsevier Academic Press.

APPENDIX

List of specimens used in this study

Puma concolor ($N = 110$). CFA: 4429; 5229; 5732; 5912; 6103; 6143; 8884; 9244; 9426; 9884; 9885; 10020; 10331; 10341; 10359; 10390; 10391; 10547; 11078; 12822. CML: 234; 235; 443; 650; 787; 788; 3726; 5483; 5485; 6197; 6338; 6354; 6355; 6356; 6357; 6358; 6359; 6363; 7252. MACN: 3.15; 4.378; 4.422; 7.39; 20.64; 24.19; 25.61; 25.152; 25.208; 26.9; 28.168; 29.240; 29.841; 30.19; 30.196; 30.214; 30.215; 30.250; 30.251; 31.57; 32.80; 36.615; 37.28; 38.44; 39.208; 47.2; 47.405; 48.344; 48.345; 49.296; 49.470; 50.46; 53.59; 53.97; 214; 13045; 13046; 13047; 13048; 13059; 13074; 13328; 13330; 13339; 13340; 13341; 13342; 13343; 13344; 13345; 13346; 13457; 13458; 13459; 13460; 13461; 13462; 14024; 15307; 19244; 20629; 20630; 23295; 23296; 24260; 24261. MLP: 31.VIII.98.2; 4.VIII.98.6; 20.IX.49.14; 1314; 1633.

Herpailurus yagouaroundi ($N = 147$). AMNH: 395; 14859; 22679; 24662; 24685; 24853; 42857; 42958; 46538; 70391; 70438; 71115; 78836; 80058; 80205; 98554; 98602; 98649; 100092; 119205; 123279; 126184; 126978; 133970; 134057; 135150; 139231; 139774; 143466; 143887; 145961; 147577; 150010; 173911; 178704; 178705; 183120; 183288; 215137. CFA: 4081; 4174; 4679; 4719; 4720; 4987; 5390; 5403; 5757; 8339; 12821. CML: 673; 1085; 2402; 3727; 4073; 6193; 6336. FMNH: 7454; 14896; 20438; 20439; 22472; 41222; 51865; 53042; 60692; 60793; 63894; 66351; 69647; 79924; 88478; 88479; 88480; 98763. MACN: 4.201; 16.8; 18.7; 30.23; 31.5; 33.4; 36.11; 36.484; 40.190; 42.373; 47.372; 50.104; 17253; 23173; 23661. MLP: 709; 737; 748; 749. NMNH: A3838; 8571; 19973; 29952; 32676; 32677; 73709; 90952; 98073; 98074; 114844; 121891; 124336; 125348; 125456; 126700; 132520; 133205; 141460; 144077; 148736; 148737; 152160; 152161; 153531; 154187; 177544; 180223; 234355; 241196; 241573; 244860; 254905; 258328; 266867; 269141; 281396; 281397; 281398; 286886; 296627; 294034; 305763; 334558; 338975; 339684; 361048; 361049; 361884; 443193; 443299; 541506; 546106.

Acinonyx jubatus ($N = 79$). AMNH: 3832; 22824; 27897; 35307; 35997; 35998; 36426; 70549; 70550; 80090; 80108; 80125; 80172; 80618; 80619; 80620; 88626; 90255; 100309; 119654; 119655; 119656;

119657; 119682; 130135; 135083; 135519; 161139; 180086. FMNH: 1445; 1453; 26900; 29633; 29634; 29635; 34589; 34669; 39475; 39476; 60060; 60421; 60447; 60535; 89918; 104598; 104810; 104980; 127834; 135073; 150779; 168874. MACN: 29.891. NMNH: 161922; 162928; 162929; 163090; 163091; 163097; 163098; 163884; 173001; 181596; 181598; 181599; 182316; 182319; 182322; 182698; 251793; 270479; 361490; 395137; 398031; 520539; 521037; 521058; 540001; 540002; 540003.

SUPPORTING INFORMATION

Additional Supporting Information may be found in the online version of this article at the publisher's web-site:

Figure S1. Box plots, including sex, of cranial Procrustes distance (A, C, E) and centroid size (B, D, F) for *Puma concolor* (A, B), *Herpailurus yagouaroundi* (C, D), and *Acinonyx jubatus* (E,F).
Table S1. Summary of results of the Mann–Whitney *U*-test for cranial allometry, between age classes and sexes, for *Puma concolor*, *Herpailurus yagouaroundi*, and *Acinonyx jubatus*.